

## Supplemental Material

### Cancer-associated mutations in human pyruvate kinase M2 impair enzyme activity

Vivian M. Liu<sup>1,2,‡</sup>, Andrea J. Howell<sup>1,‡</sup>, Aaron M. Hosios<sup>1</sup>, Zhaoqi Li<sup>1</sup>,

William J. Israelsen<sup>1,3\*</sup>, Matthew G. Vander Heiden<sup>1,4\*</sup>

<sup>1</sup>David H. Koch Institute for Integrative Cancer Research, Massachusetts Institute of Technology, Cambridge, Massachusetts, 02139, United States

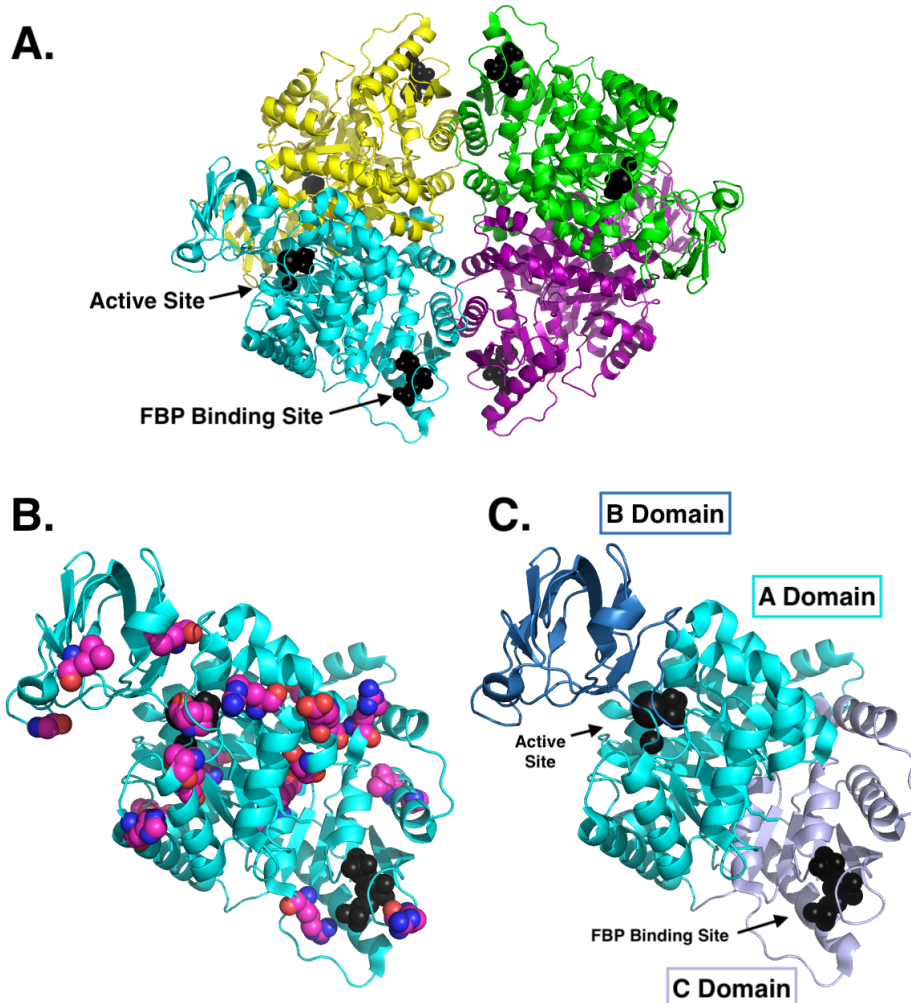
<sup>2</sup>Harvard-MIT Health Sciences and Technology Division, Harvard Medical School, Boston, MA 02115, United States

<sup>3</sup>Department of Biochemistry, University of Texas Southwestern Medical Center, Dallas, TX 75390, United States

<sup>4</sup>Dana-Farber Cancer Institute, Boston, MA 02115, United States

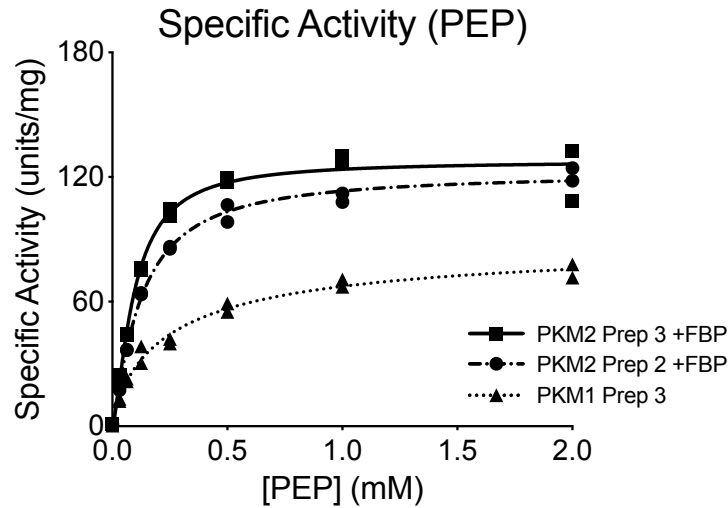
<sup>‡</sup>Equal contribution

\*



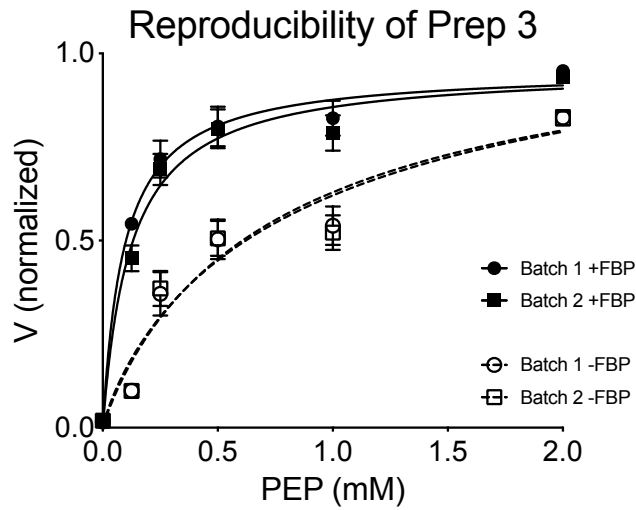
**Supplemental Figure 1. Structural Location of Cancer Mutations.**

(A) The structure (PDB: 3BJF [23]) of a PKM2 tetramer is shown with each subunit in a different color . The active site and FBP binding site are bound by ligands in this structure; these are shown as black spheres. (B) The residues affected by 23 mutations reported in The Cancer Genome Atlas (TCGA) are shown as colored spheres in the cyan subunit, except for F12 which is not visible in this structure (see also Figure 3). The ligands bound at the active site and FBP binding site are shown as black spheres. (C) The same subunit is highlighted in different shades of color to show the three main domains of the enzyme. The ligands bound at the active site and FBP binding site are shown as black spheres.



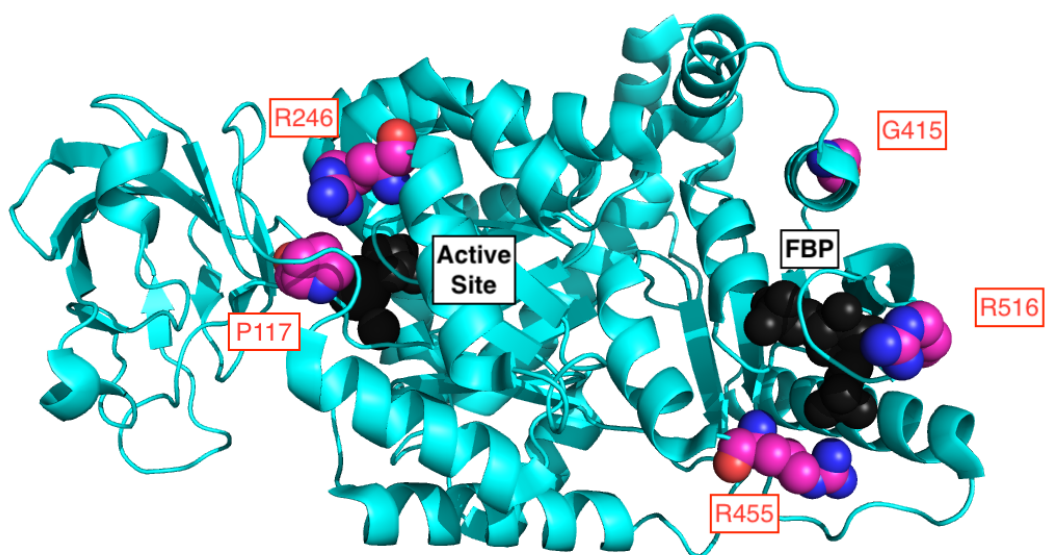
**Supplemental Figure 2. PKM2 Prepared via a Two-Column Method (Prep 3) and Refolding (Prep 2) Have Comparable Specific Activities.**

Wild-type PKM2 prepared via the refolding method (Prep 2) has specific activity similar to that of native enzyme purified via a two-column method (Prep 3). The PKM2 Prep 3 curve shown here is the same data as Figure 2A. PKM1 is shown for comparison. The kinetic assays were performed with varying concentrations of PEP and saturating (5 mM) ADP. FBP was present at 2 mM as indicated in the legend.



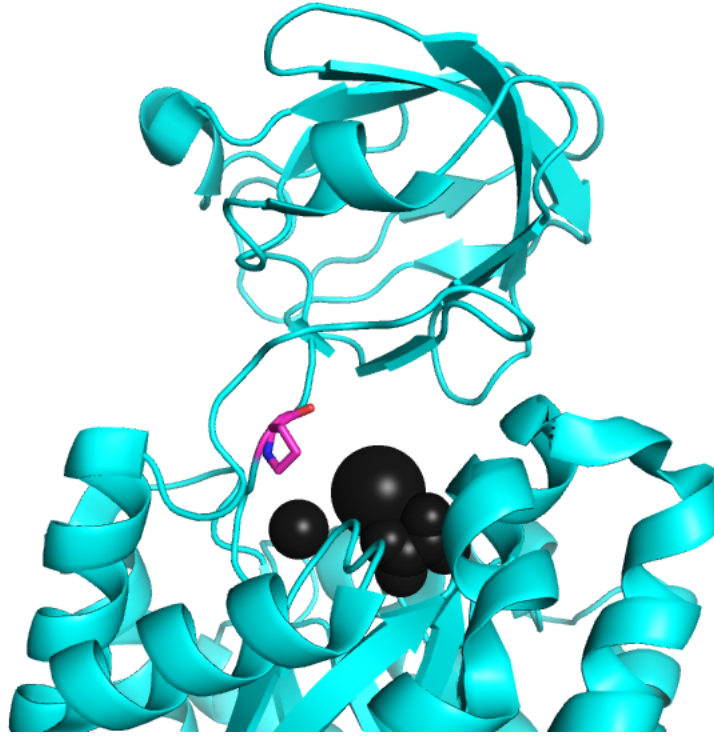
**Supplemental Figure 3. Prep 3 Allows Reproducible Kinetic Results from Independent Batches of WT PKM2.**

Two independent batches of wild-type PKM2 were prepared using the Prep 3 method. Both batches of enzyme were assayed for steady-state kinetics on the same day and the results demonstrated good agreement between batches. ADP concentration was held constant at 2 mM. Assays were performed in triplicate with and without saturating FBP. Mean and SD are shown. Fit lines are Michaelis-Menten (+FBP) and allosteric sigmoidal (-FBP).



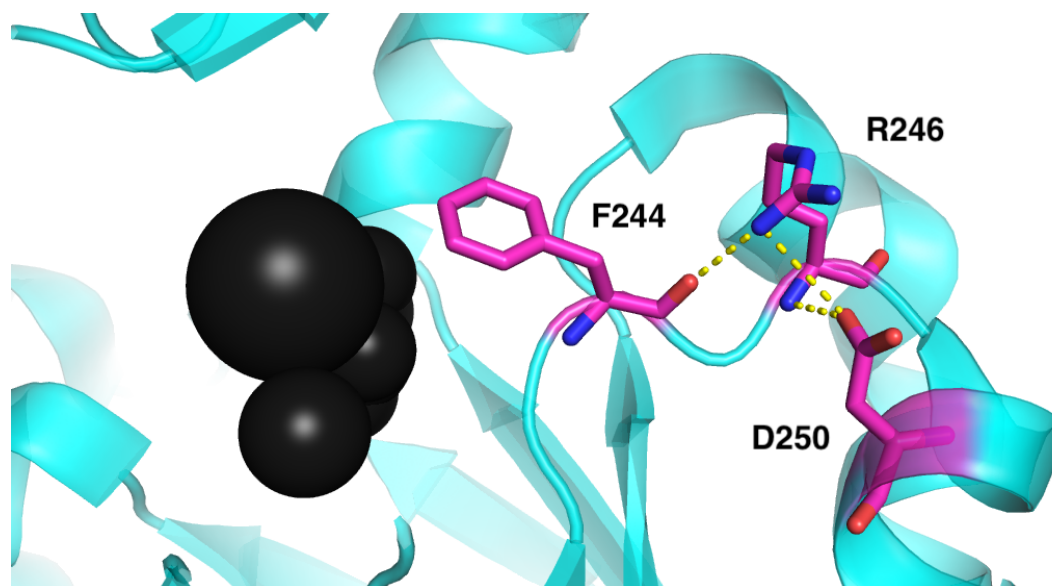
**Supplemental Figure 4. Structural Location of Cancer Mutations Addressed in this Study.**

The structure (PDB: 3BJF [23]) of one subunit of a PKM2 tetramer is shown in cyan, with bound ligands depicted as black spheres; FBP occupies its binding site and the enzyme active site is occupied by oxalate (substrate mimetic),  $Mg^{2+}$ , and  $K^+$ . The amino acids changed by the cancer mutations addressed in this paper are labeled and shown as colored spheres.



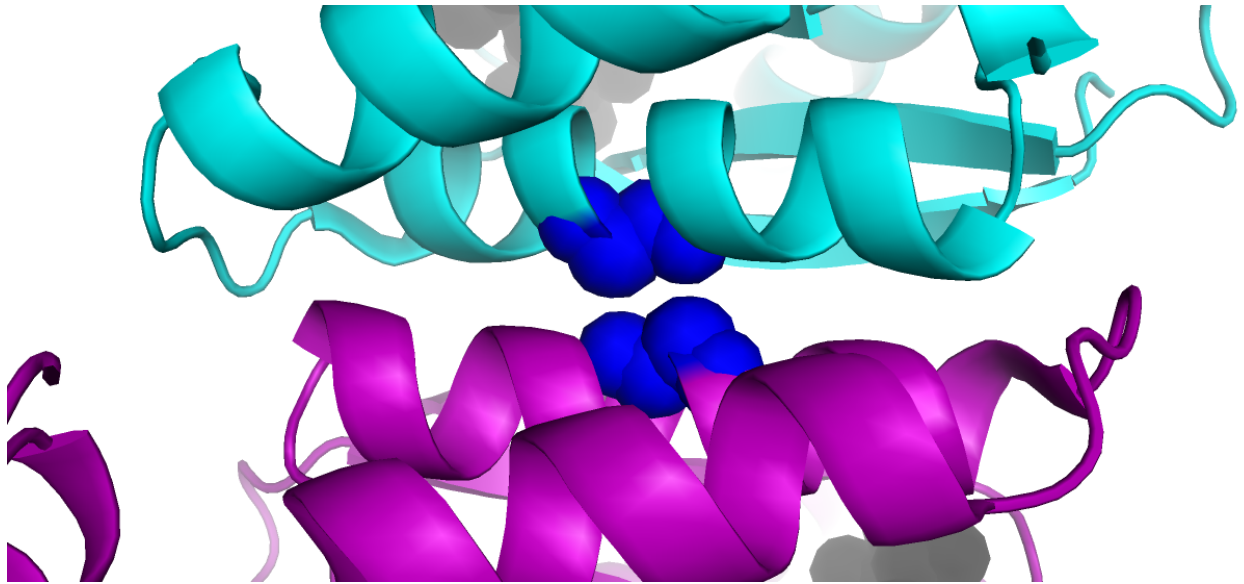
**Supplemental Figure 5. The P117L Mutation Affects the “Hinge” Allowing Active Site Closure.**

The structure (PDB: 3BJF [23]) of one subunit of a PKM2 tetramer is shown in cyan, with bound ligands in the active site (oxalate, Mg<sup>2+</sup>, and K<sup>+</sup>) depicted as black spheres. The highly-conserved proline 117 is depicted in magenta; this residue found the hinge region that allows closure of the B domain (top) down onto the active site, which is hosted in the A domain.



**Supplemental Figure 6. The R246S Mutation Putatively Disrupts Structural Contacts Near the Active Site.**

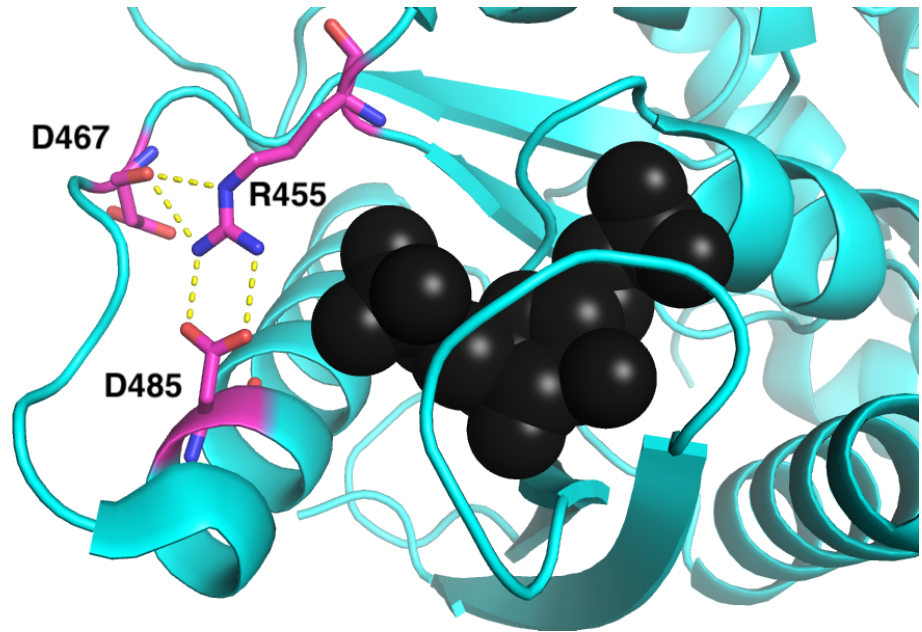
The structure (PDB: 3BJF [23]) of one subunit of a PKM2 tetramer is shown in cyan, with bound ligands in the active site (oxalate, Mg<sup>2+</sup>, and K<sup>+</sup>) depicted as black spheres. Arginine 246 makes contacts with the side chain of glutamate 250 and the backbone oxygen of phenylalanine 244. Loss of these contacts in the R246S cancer mutations may result in structural changes at or near the active site of the enzyme.



**Supplemental Figure 7. The G415R Mutation Putatively Disrupts Tight Packing at the Dimer-Dimer Interface.**

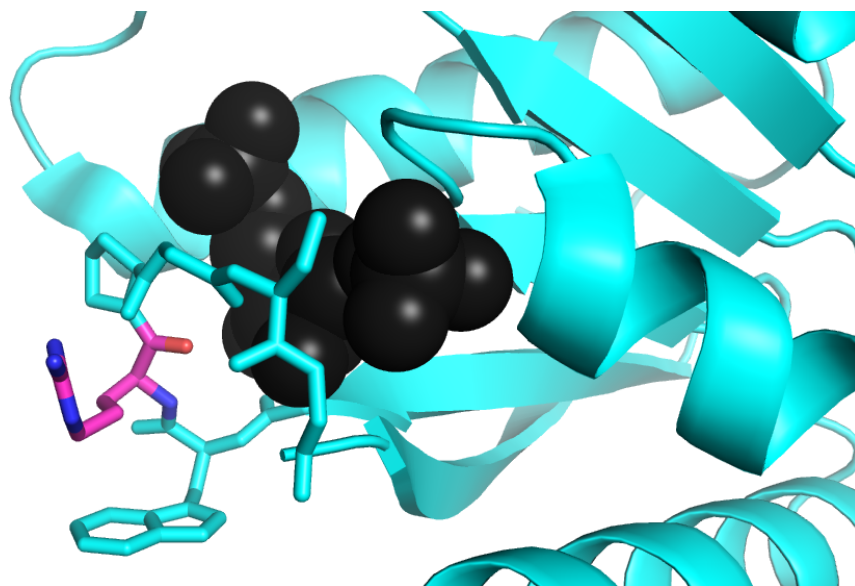
The dimer-dimer interface of PKM2 (PDB: 3BJF [23]) is shown with two different subunits shown in cyan and magenta. The G415 residues from each subunit are shown as blue spheres. The small hydrogen side chain of G415 allows for tight packing of the  $\alpha$ -helices at the dimer-dimer interface. Substitution of glycine with bulky, positively-charged arginine in the cancer mutation presumably disrupts the normal association of the subunits via steric hindrance and charge repulsion.





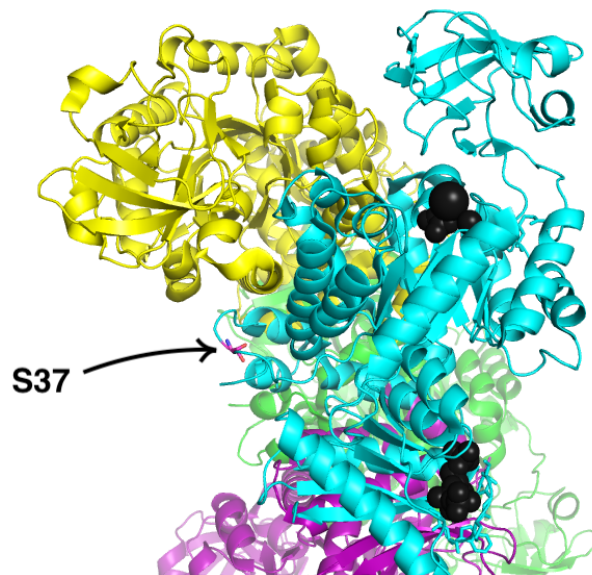
**Supplemental Figure 8. The R455Q Mutation Putatively Disrupts Structural Contacts near the FBP Binding Site.**

The FBP binding site of one subunit of a PKM2 tetramer is shown (PDB: 3BJF [23]). The protein structure is cyan, with FBP depicted as black spheres and relevant residues shown in magenta. While R455 does not interact directly with FBP, this residue makes structural contacts in this region of the protein; the R455Q mutation eliminates the positive charge of this residue and presumably disrupts the contacts with D467 and D485.



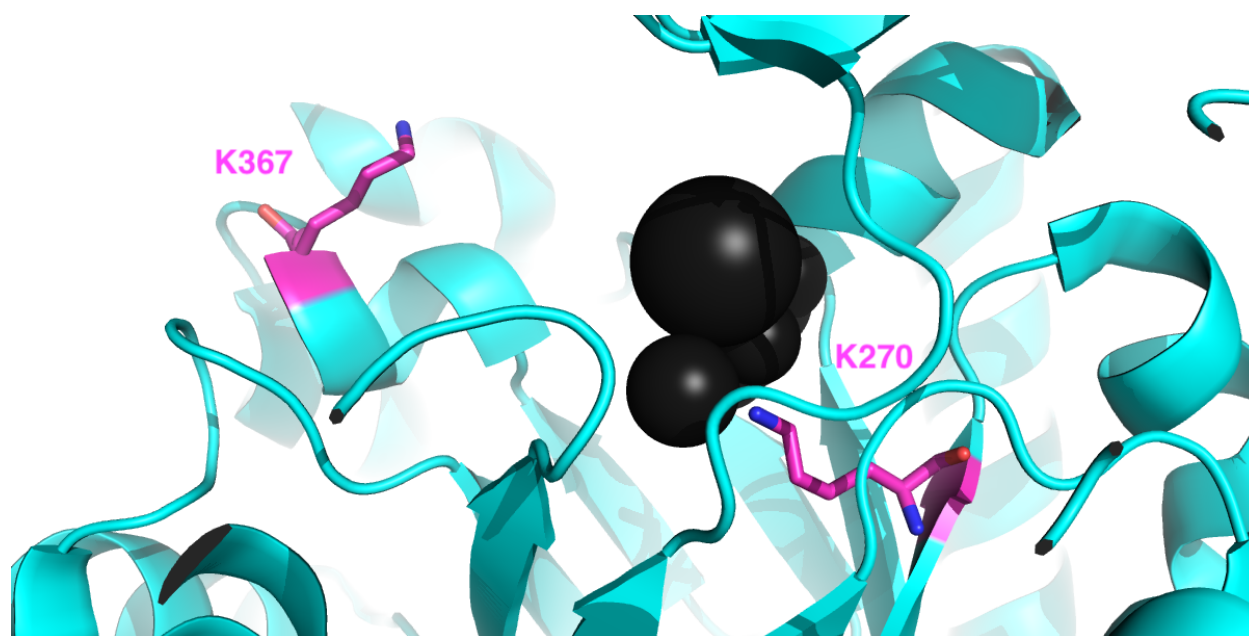
**Supplemental Figure 9. The R516C Mutation is Located on the FBP Binding Loop.**

The FBP binding site of one subunit of a PKM2 tetramer is shown (PDB: 3BJF [23]). Bound FBP is depicted as black spheres. The binding loop residues are shown as stick models, with R516 highlighted in magenta. The R516C cancer mutation results in a change of charge on the FBP binding loop and presents a possible solvent-exposed reactive cysteine.



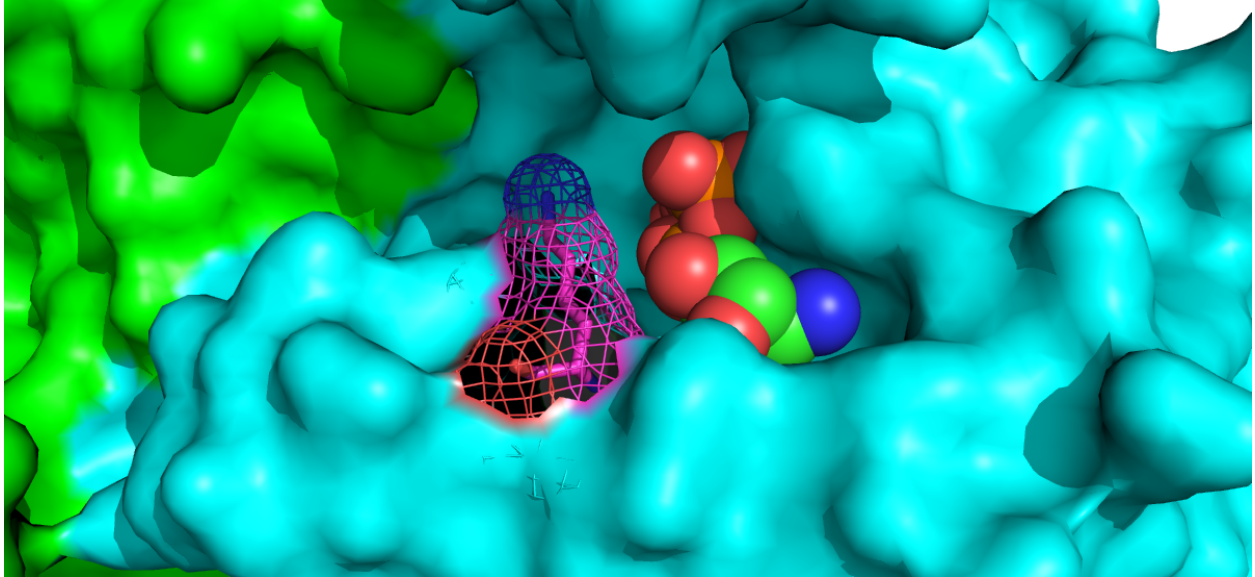
### Supplemental Figure 10. S37 is Solvent Exposed

The structure (PDB: 3BJF [23]) of a PKM2 tetramer is shown with each subunit in a different color. The active site and FBP binding site are occupied by ligands, which are shown as black spheres in the cyan subunit. Serine 37 found on the cyan subunit is colored magenta for contrast; this residue is solvent exposed.



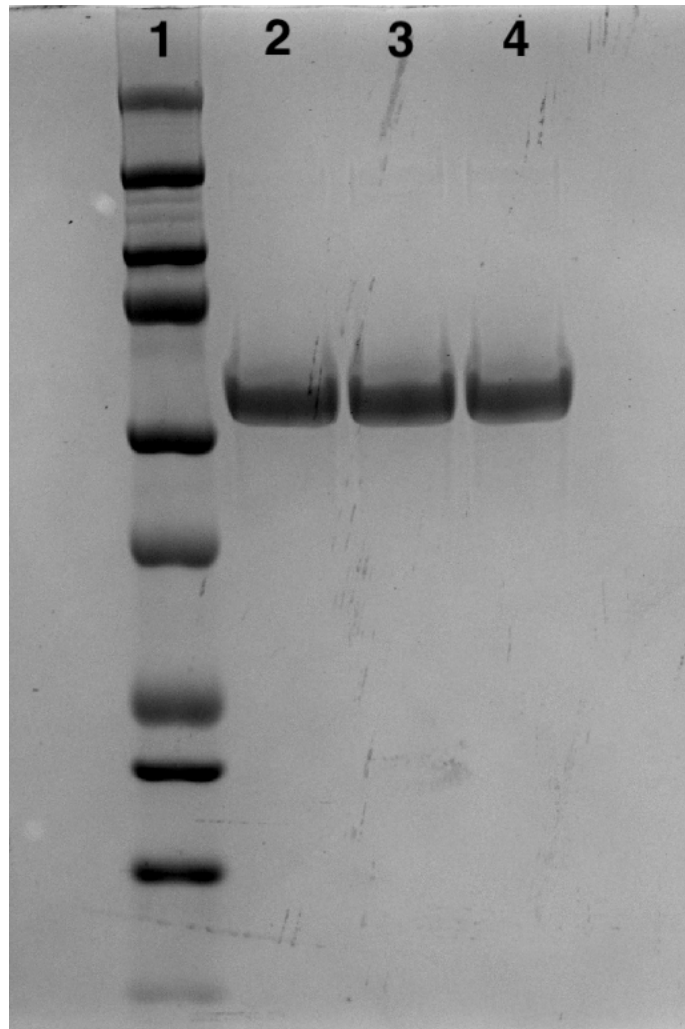
**Supplemental Figure 11. Residues K270 and K367 Lie in the Active Site**

The active site of one subunit of a PKM2 tetramer is shown, with (PDB: 3BJF [23]). Residues of interest are colored for contrast and shown as stick models. The active site is occupied by oxalate (substrate mimetic),  $Mg^{2+}$ , and  $K^{+}$ , which are shown as black spheres. The side chain of K270 is positioned to perform catalysis, while K367 lies near the ADP binding site.



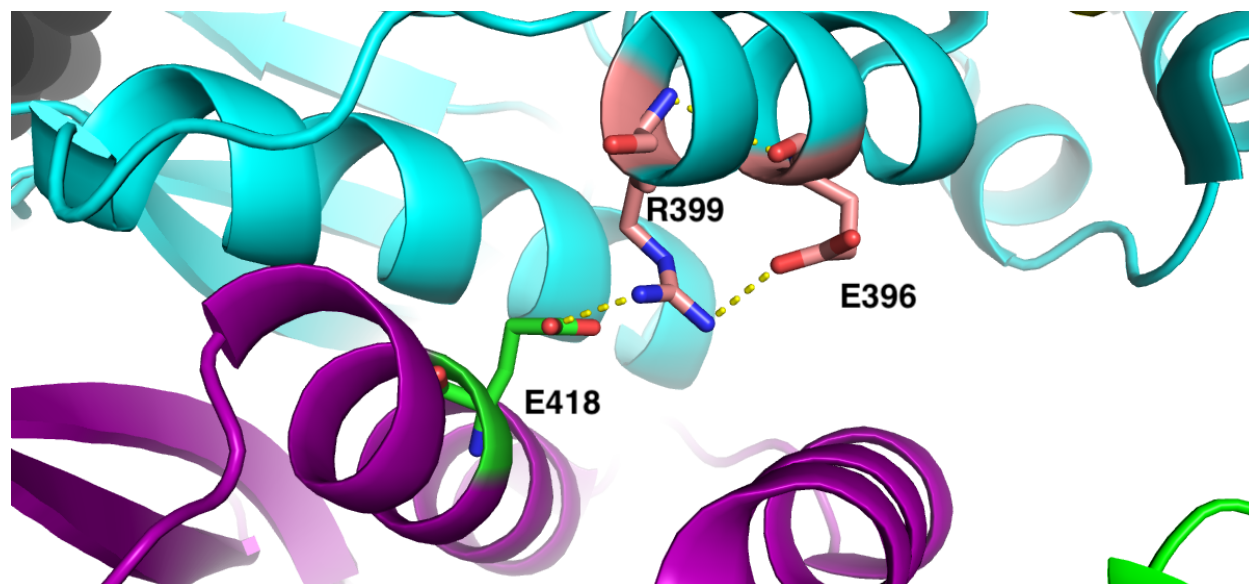
**Supplemental Figure 12. K367 Is Near the ADP Binding Site but Does Not Contact Bound Substrate**

One active site of a PKM2 tetramer is shown (PDB: 3GR4, unpublished). The surface of two subunits is visible; one subunit is cyan, the other is green. Lysine 367 (K367) is depicted as a stick model underneath surface mesh. This residue lies near to the bound ADP, which is shown as colored spheres. K367 is near to, but does not contact, bound ADP in this structure.



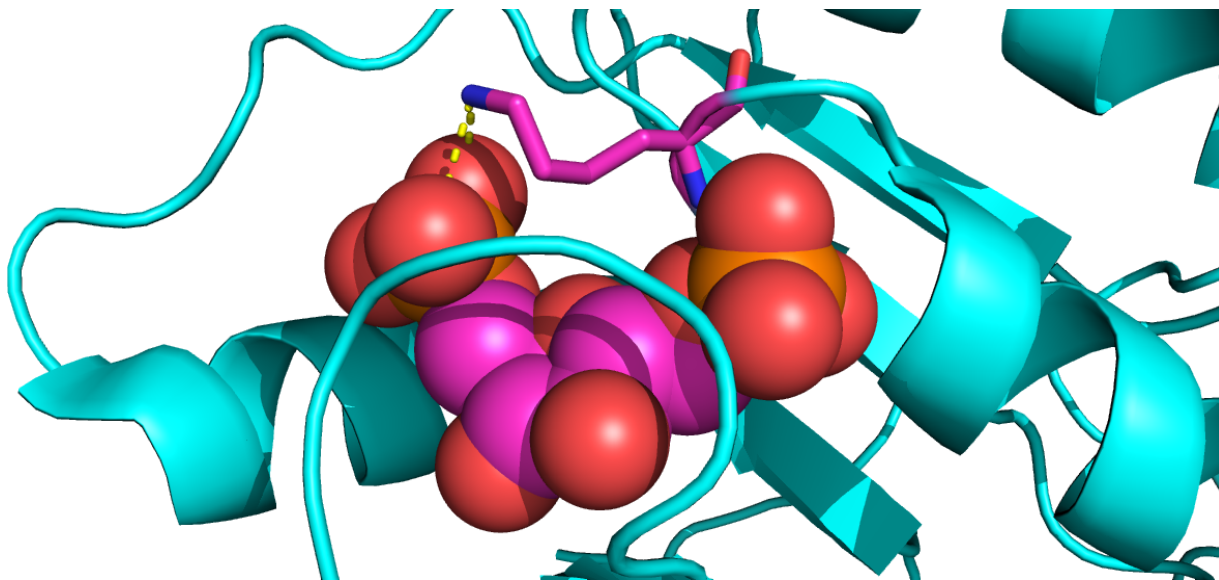
**Supplemental Figure 13. PKM2 Mutants With Reduced Activity Are Effectively Prepared Via Prep 3.**

PKM2, PKM2 K270M, and PKM2 K367M proteins were prepared via the two-column method (Prep 3), separated by SDS-PAGE and stained with Coomassie Brilliant Blue. Lane 1, Molecular Weight Ladder; Lane 2, PKM2 WT (5  $\mu$ g); Lane 3, PKM2 K270M (5  $\mu$ g); Lane 4, PKM2 K367M (5  $\mu$ g).



**Supplemental Figure 14. The R399E Mutation Disrupts Favorable Ionic Contacts at the Dimer-Dimer Interface.**

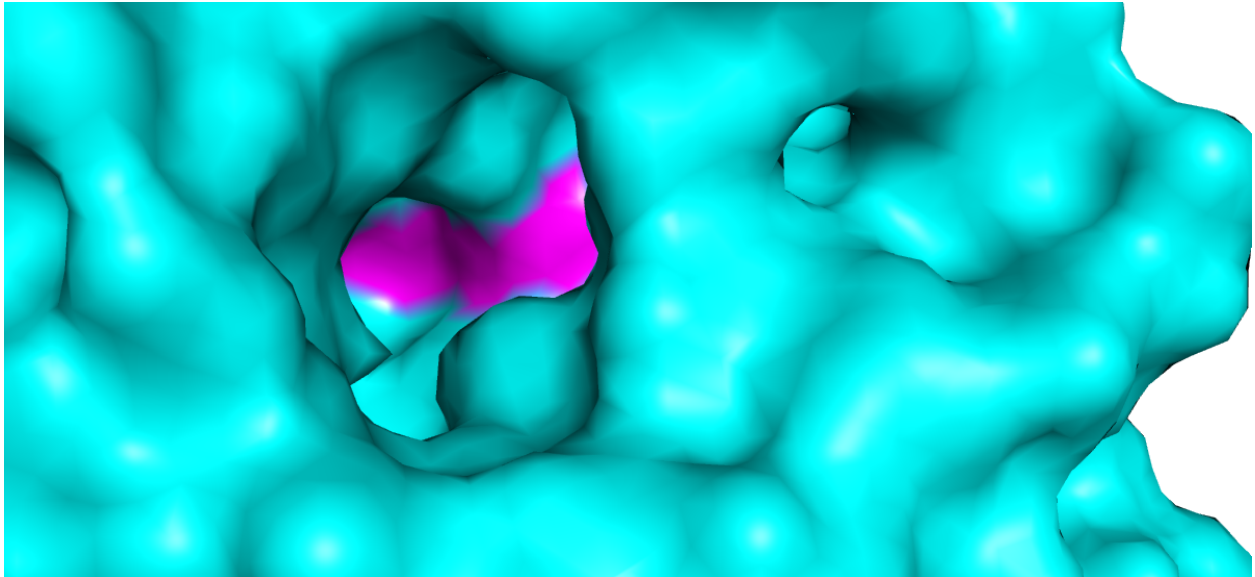
A portion of the dimer-dimer interface of a PKM2 tetramer is shown, with one subunit in cyan and the opposing subunit in magenta (PDB: 3BJF [23]). Residues of interest are colored for contrast and shown as stick models. Positively charged residue R399 is sandwiched between the negative charges of E396 on same chain and E418 on the opposing subunit. Charge reversal caused by the R399E mutation likely disrupts favorable inter-subunit contacts.



**Supplemental Figure 15. The K433E Mutation Disrupts the FBP-K433 Interaction**

The FBP binding site of one subunit of a PKM2 tetramer is shown (PDB: 3BJF [23]) . Bound FBP is depicted as colored spheres. The K433 residue is shown as a colored stick model. The positively-charged K433 side chain interacts with a negatively-charged phosphate group of FBP, and the K433 residue helps to enclose FBP in the binding pocket. The charge reversal caused by the K433E mutation causes electrostatic repulsion and disrupts FBP binding.





**Supplemental Figure 16. H464 is Located in the Binding Pocket of Serine, Alanine, and Phenylalanine**

The surface of interface of a PKM2 tetramer is shown cyan (PDB: 3BJF [23]). The surface of histidine 464 is colored magenta and located deep in a pocket that is a known binding site for serine, alanine, and phenylalanine.

**Supplemental Table 1. Missense Cancer Mutations of PKM2 Examined in this Study**

| <b>Mutation</b> | <b>TCGA Center</b> | <b>No. of Occurrences</b> | <b>Cancer Type</b>  |
|-----------------|--------------------|---------------------------|---------------------|
| P117L           | WashU              | 5                         | Uterine             |
| R246S           | Broad              | 3                         | Lung Adenocarcinoma |
| G415R           | Baylor             | 1                         | Kidney              |
| R455Q           | WashU              | 5                         | Uterine             |
| R516C           | WashU              | 5                         | Uterine             |